Development of a Novel Fetal Heart Rate Monitor for Twin Pregnancies

A Technical Report submitted to the Department of Biomedical Engineering

Presented to the Faculty of the School of Engineering and Applied Science

University of Virginia • Charlottesville, Virginia

In Partial Fulfillment of the Requirements for the Degree

Bachelor of Science, School of Engineering

Spring, 2025

Technical Project Team Members

Anqi Wu

Anita Kau

Rola Suleiman

On my honor as a University Student, I have neither given nor received unauthorized aid on this assignment as defined by the Honor Guidelines for Thesis-Related Assignments

Advisor

Kristen Naegle, Department of Biomedical Engineering

Natasha Sheybani, Department of Biomedical Engineering

Natasha Sheybani May 6, 2025

DocuSigned by:
Kristen Naegle 5/6/2025
E6594665A827496...

Development of a Novel Fetal Heart Rate Triangulation Algorithm for Twin Pregnancies

Anqi Wu[a,1*]. Anita R. Kau[a,2*], Rola R. Suleiman[a,3*], Andrew Thede[a,4], Dr. Natasha Sheybani[a,5], Dr. Kristen Naegle[a,6]

[a] Department of Biomedical Engineering
[1] Correspondence: pmx5pm@virginia.edu
[2] Correspondence: ypm2cv@virginia.edu
[3] Correspondence: cnq8zk@virginia.edu
[4] Correspondence: att9gw@virginia.edu
[5] Correspondence: nds3sa@virginia.edu
[6] Correspondence: kmn4mj@virginia.edu

* Authors contributed equally

Abstract

Twin births make up approximately 98% of all multiple births in the U.S., yet they carry nearly four times the infant mortality rate and double the maternal mortality rate of singleton pregnancies. A major contributing factor is that current Doppler-based fetal monitoring systems cannot reliably separate two fetal heartbeats when their signals overlap, potentially delaying life-saving interventions. To address this, we developed a custom sensing system and signal processing pipeline capable of both separating and localizing two fetal heart sources. We tested the system using a hydrogel phantom embedded with two small speakers playing real fetal heart recordings. Signals were collected with five contact-based vibration sensors and filtered to isolate the 90–180 bpm range. We applied a Gaussian Mixture Model to cluster heartbeats based on time-difference-of-arrival (TDOA) features and used multilateration to estimate source positions. Our results showed lower heart rate error when the FHRs were distinctly different or nearly identical but performance declined around 110 bpm, likely due to increased signal overlap and noise. Localization accuracy averaged 6–8 cm, with better results for sources closer to the sensor array centroid. This work demonstrates the feasibility of differentiating and spatially resolving fetal heart signals in twin scenarios. Future development will include integration of maternal heart signals and transitioning toward a wearable device for clinical use.

Keywords: Fetal heart rate, gel phantom, multiple gestation pregnancy

Introduction

Twin births account for around 98% of all multiple gestations within the United States.[1] These births experience an infant mortality rate that is nearly 4 times higher than for single births.[2] Additionally maternal mortality is twice as high when delivering twins (0.75%) compared to single deliveries (0.37%).[3] While there are many factors that lead to these statistics, a major reason is the lack of accurate and efficient monitoring for multiple gestation births. The current industry standard commonly used in modern clinical practice for monitoring fetal heart rate (fHR) is Doppler ultrasound (US). Doppler US works by measuring the distance a reflection of US waves travel through mediums over time. While it has been the industry standard for quite some time, it possesses many limitations and issues. Not only does the device typically obstruct the lower back, making it difficult for doctors to administer medication during labor and delivery, but it also is unable to accurately and efficiently measure the two fHR as distinct signals. Both hearts share the same transducer sample volume, which causes an inability for DUS to differentiate the fHR signals clearly and leads to inaccurate fHR readings. Taking all these problems into consideration, this project sought to design a hydrogel phantom system that mimics the environment of a pregnant person with a multiple gestation pregnancy. Using this gel phantom system, the developed algorithm could then collect the data and differentiate the signals to present them as distinct fHR and also accurately determine their locations.

Significance

Around 70% of twin births are premature, resulting in higher rates of neonatal and fetal deaths from multiple gestations in comparison to singletons.[4] It is crucial that doctors and the entire healthcare team is able to use fHR monitoring to properly and accurately assess the health of the fetuses through each gestation period. One issue with the current DUS technology is the inability to reliably differentiate the individual heartbeats until 10-12 weeks of gestation.[5] This makes it difficult for doctors to catch fetal health complications early on and intervene to address them. Additionally, multiple gestations naturally means that the womb is a crowded space, with the positioning of the fetuses close to one another especially in the later gestations. This further complicates the signal differentiation and ability of clinicians to determine which baby is where and which fHR belongs to which fetus. As such, accurate monitoring of fHR in multiple gestations is both necessary and crucial to ensure the healthy delivery of twin babies. The results from this project focused on modeling two stationary fetuses will provide an informative foundation for further development of the system and monitor. Developing this novel fHR monitor for multiple gestations will improve accuracy of twin monitoring during pregnancy. This will better inform physicians and health care teams on how to best care for the babies once they are delivered, and if needed, intervene early on to prevent complications. While fHR monitors are common in the clinical setting already, devices that accurately differentiate between multiple heart rates and eliminate background noise have not been previously implemented. Considering that multifetal gestations are not only on the rise, but that multiple gestations are also associated with increased incidence of preterm labor and delivery, our novel monitor would enable physicians to better understand the health status of the fetuses and intervene as necessary to ensure delivery of healthy babies.

Specific Aim 1

We aim to design a hydrogel phantom to mimic the uterus with multiple fetuses. This would be achieved by first constructing a hydrogel phantom system with two speakers representing the two fetal heartbeats, minimizing undesired signal noise by inserting the speakers in a non-invasive manner through the use of molds. In order to collect the wave frequency from speakers with the least signal noise, we would use a circular array of seven piezoelectric sound vibration detectors, placed in a design similar to previous designs of fHR monitors. The hydrogel phantom would then be connected to an electric system that is constructed to take the wave frequency collected by the piezoelectrics as input for the Arduino interface.

Specific Aim 2

In order to ensure that each distinct fHR could be detected, we aimed to separate the adjacent heartbeat signals with low error rate. Signals generated by the speakers would be obtained and collected. The signals would then be processed through a bandpass filter, amplified, before mathematically determining the position of the heart beats. Once this was completed, a triangulation algorithm in MATLAB would be implemented to calculate the physical distances separating each sensor to the heartbeat based on the detection time of piezoelectric sensors placed at different locations allowing for differentiation of the unique modeled heart rate signals in the gel phantom system. This would also help ensure greater accuracy in determination of heartbeat positions. Errors would be detected by comparing the piezoelectric sensor's signal to the original speaker signal, and this information used to optimize the signal-to-noise ratio to ensure accurate output and differentiation.

Specific Aim 3

The final aim was to evaluate the accuracy of fHR measurement data outputted by the novel design. To do so, the design would be tested with the two speakers emitting a known frequency of sound and placed at 3 different distances from each other. The mock fHR data resulting from using a standard DUS would be collected in order for us to compare our device with the industry standard. Lastly we would test this novel design with two speakers fixed at a certain distance. The accuracy of this novel design and the clinical standard DUS would then be compared.

Materials

Gel Phantom Material

The gel phantom was created using Gelatin #3 purchased from Humimic Medical. Since this device would be used to monitor fHR during pregnancy, we wanted to mimic this environment as closely as possible. As such, Humimic Medical Gel Gelatin #3 was selected for its ability to replicate the acoustic properties of biological tissue, ensuring that mocked fetal heartbeat signals emitted by the speakers propagate through it in a manner similar to twins *in utero*. To create the hydrogel phantom, we melted the gel in a convection oven, using an oven-safe baking dish as the mold. The baking dish was chosen due to its thickness being similar to that of the uterine lining which is 12 ± 3 mm.[6]

Gel Phantom Fetal Heartbeat System

An Arduino Uno was purchased and utilized to develop our speaker system that would generate the fHR. Two oven-safe speaker molds made using resin were placed in the gel phantom during baking and replaced with the actual two 3 Watt 8 Ohm speakers purchased from Amazon when solidified. These speakers, embedded within the hydrogel phantom, each emitted distinct fHR audio files, driven by DFPlayer Mini MP3 modules, to simulate different fHR, allowing for simultaneous detection of multiple heartbeat signals.

Fetal Heart Rate Device

The fetal heartbeat sound files played through the speakers are recordings of real ultrasound fetal heartbeats, sourced from YouTube. Links to these recordings are provided in Supplementary Material X. The five piezoelectric sensors, along with their corresponding wires and extenders used in the fHR device, were purchased from Amazon. A complete list of vendors is also included in Supplementary Table 2.

Methods

Gel Phantom Development

Two speakers were successfully molded and cast using silicone rubber molds and air-hardening resin to create durable and precisely shaped components. The molded speakers were securely taped at the bottom of a pan to ensure proper alignment and mechanical stability during the subsequent gel phantom fabrication process.

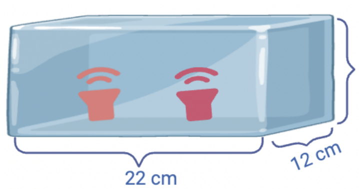

Fig. 1. Hydrogel Phantom Dimension. The quantity of material and the dimensions of the dish were selected to produce a final phantom measuring approximately 2 cm in height, 22 cm in length, and 12 cm in width.

To integrate the speakers with the acoustic medium, Humimic Gelatin gel was prepared and cast over the embedded speakers. A total of 1.5 pounds of gel phantom material was used. Following manufacturer guidelines, the gel was first cut into approximately 1-inch-sized pieces using scissors and placed into an oven-safe dish lined with aluminum foil. The gel material was melted by placing the dish in a conventional oven at 250°F (125°C) for 4 hours. After heating, the phantom was removed from the oven and allowed to cool and solidify at room temperature for 12 hours prior to use. The finished hydrogel system was 22 cm long by 12 cm wide by 2 cm tall as depicted in Figure 1.

Piezoelectric Sensor Array Development

The fetal heart rate (FHR) monitor was developed using an Arduino Mega 2560 microcontroller to power and collect data from five piezoelectric sensors, each connected to separate analog voltage input pins. The five sensors were mounted in a non-collinear, randomized array within the hydrogel phantom, with the following coordinates (in centimeters): (9.0, 8.5), (11.7, 15.5), (3.5, 2.5), (2.5, 11.5), and (5.0, 18.5). A non-collinear and randomized sensor arrangement was specifically chosen to improve source localization accuracy by minimizing geometric degeneracy and reducing systematic bias. Regular, collinear sensor layouts can produce ambiguities in time difference of arrival (TDOA) localization, as hyperbolic intersections can collapse onto similar lines; randomized positioning improves spatial resolution and robustness of the localization algorithm.

Each piezoelectric sensor was wired with its positive (red) lead connected to an analog input pin (A1–A5) on the Arduino, and its negative (black) lead connected to ground. The positive lead was connected to ground through a 1 MΩ resistor. This connection stabilized the voltage signal and suppressed floating noise.

Two speakers embedded in the gel phantom were driven by separate DFPlayer Mini MP3 modules (GD3300-based), which were controlled by the Arduino Mega via serial communication. For MP3 Player 1, the DFPlayer's TX pin was connected to the Arduino’s RX2 (Pin 17) and its RX pin connected to TX2 (Pin 16); for MP3 Player 2, the TX and RX pins were connected to RX1 (Pin 19) and TX1 (Pin 18), respectively. Power (VCC) and

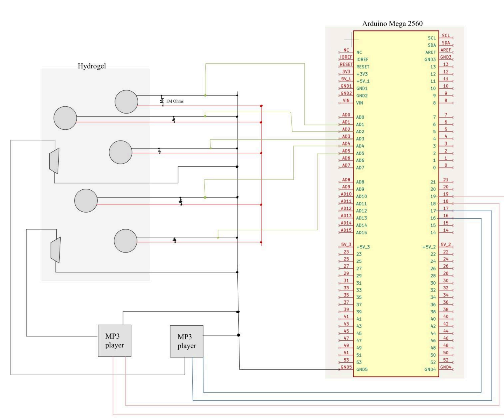

Fig. 2. Circuit Diagram of Piezoelectric Array Sensors and Speakers Set Up. Five piezoelectric sensors were embedded in a randomized array within the hydrogel phantom and connected to analog input pins (A1–A5) on the Arduino Mega 2560. The entire circuit, including the Arduino and MP3 players, was powered through a single USB connection to a computer.

ground (GND) pins of each DFPlayer module were connected to the Arduino's 5V and GND outputs. The speaker terminals (SPK1 and SPK2) of the DFPlayer were connected directly to the positive and negative terminals of the corresponding embedded speakers. (Figure 2)

Fetal Heart Rate Monitor Testing

Ten trial conditions were conducted by pairing synthetic fetal heart rate (FHR) signals at different frequencies. The tested combinations involved FHR1 (147 bpm, 2.45 Hz), FHR2 (172 bpm, 2.867 Hz), FHR3 (142 bpm, 2.375 Hz), and FHR4 (110 bpm, 1.833 Hz), including all identical and non-identical pairings among these signals. Each numeral corresponds to a distinct FHR frequency. Each trial condition was repeated three times to assess consistency and variability. This design enabled evaluation across conditions featuring identical and distinctly separated heart rates.

Data Collection

To acquire time-resolved voltage data from the piezoelectric sensor array, a real-time serial communication and logging system was developed. Data was streamed from the Arduino microcontroller via a USB connection at a baud rate of 9600 and recorded continuously for 35 seconds for each of the 30 simultaneous heartbeat trials. Each serial transmission contained analog voltage readings from five piezoelectric sensors along with a corresponding timestamp measured in microseconds. Upon receipt, raw analog-to-digital converter (ADC) values (ranging from 0 to 1023) were converted to voltage measurements using a reference voltage of 5.0 V. Timestamps were simultaneously rescaled from microseconds to seconds to ensure consistency in subsequent analyses. The processed data were written directly to a comma-separated values (CSV) file, with each row representing the voltage output of all sensors at a discrete time point. To ensure data integrity, the script incorporated validation checks on the format of each incoming line, discarding any corrupted or improperly formatted entries. This system enabled synchronized, high-resolution acquisition of multi-sensor voltage signals, providing the raw dataset necessary for downstream signal filtering and frequency-domain characterization.

Fetal Heart Rate Peak Detection

The data were first preprocessed by discarding the initial 7 seconds to remove potential artifacts. Peak detection was performed on the reference sensor, using a threshold set at 30% of its maximum amplitude to eliminate non eligible peaks that are potential artifacts. Around each detected peak, short signal windows of ±35 samples (i.e., a total window size of 70 samples) were extracted across all sensors.

Time Difference of Arrival (TDOA) Estimation via Cross-Correlation

Time differences of arrival (TDOAs) between sensors were estimated using cross-correlation analysis applied to short signal segments surrounding detected peaks. For each identified peak in the reference sensor, a symmetric time window of ±35 samples was extracted from all sensor channels. Short signal windows were used to minimize the influence of signal nonstationarities, noise, and overlapping events, ensuring that the cross-correlation focused on the local structure of each peak. Within each window, the reference sensor (Piezoelectric sensor #1) signal was designated as the template, and cross-correlation was performed between the reference signal and the corresponding segment from each of the other sensors. The lag corresponding to the maximum cross-correlation value was identified, representing the relative delay between the signals. This lag was then converted to time units by dividing by the sampling frequency (fs). The sampling frequency (fs) was estimated by taking the inverse of the mean time difference between consecutive timestamps. The reference sensor was assigned a TDOA of zero by definition. This procedure was repeated across all detected peaks, and the resulting TDOA estimates were averaged to obtain a robust mean TDOA vector for each sensor relative to the reference. This mean TDOA vector served as the input for subsequent signal reconstruction and source localization analyses.

Fetal Heart Rate Differentiation

The extracted TDOA features were then standardized and clustered using a two-component Gaussian Mixture Model (GMM) to differentiate signals originating from the two distinct sources. For each cluster, signals were realigned based on their respective TDOAs and reconstructed using envelope-weighted delay compensation to enhance signal separation.

The reconstructed cluster signals were transformed into the frequency domain using the real-valued Fast Fourier Transform (rFFT). The resulting magnitude spectra were smoothed via a Savitzky-Golay filter applied to the Hilbert-transformed envelopes. Dominant frequencies were identified by peak detection within the smoothed spectra. To ensure consistent cluster labeling across trials, clusters were reordered such that Cluster 0 corresponded to the lower dominant frequency.

Fetal Heart Source Localization

Source localization for each separated signal cluster was performed based on the estimated TDOAs. Two approaches were applied sequentially. First, source localization was attempted using nonlinear least-squares multilateration. In this approach, the estimated position of each source was determined by minimizing the sum of squared residuals between the measured and predicted time differences of arrival (TDOAs) across the array of piezoelectric sensors.

The measured TDOAs were previously obtained by performing cross-correlation analysis on short windows of the recorded signals centered around detected peaks. The final measured TDOA vector was calculated by averaging the time delays across all detected peaks.

For a given source position estimate, the predicted TDOA between any sensor and the reference sensor was computed based on the difference in Euclidean distances, divided by the assumed constant sound speed of 162,900 cm/s within the hydrogel medium. Specifically, the expected TDOA between sensor i and the reference sensor was calculated as:

$$Expected\,TDOA_i = \frac{d_i - d_{ref}}{v}$$

where d_i and d_{ref} are the distances from the source to sensor i and the reference sensor, respectively, and v is the speed of sound.

The objective function minimized the sum of squared differences between the predicted TDOAs and the experimentally measured TDOAs. An initial guess for the source location was set to the centroid of the sensor array to encourage convergence. Optimization was performed using the L-BFGS-B ("Limited-memory Broyden–Fletcher–Goldfarb–Shanno with Bound constraints") algorithm, which efficiently handles bounded nonlinear problems. Successful convergence resulted in an estimated (x, y) coordinate for the source.

If multilateration failed to converge, a grid search method was used as a fallback. Candidate positions were systematically evaluated across a predefined region (2–20 cm in x, 2–12 cm in y), and the location minimizing the total TDOA error was selected. Estimated source coordinates were reported separately for each cluster, corresponding to the separated fetal heart rate sources.

Results

Data Filtering

To enhance signal quality and isolate relevant physiological frequencies, a two-stage filtering process was applied to the raw piezoelectric sensor data. Initially, a

a

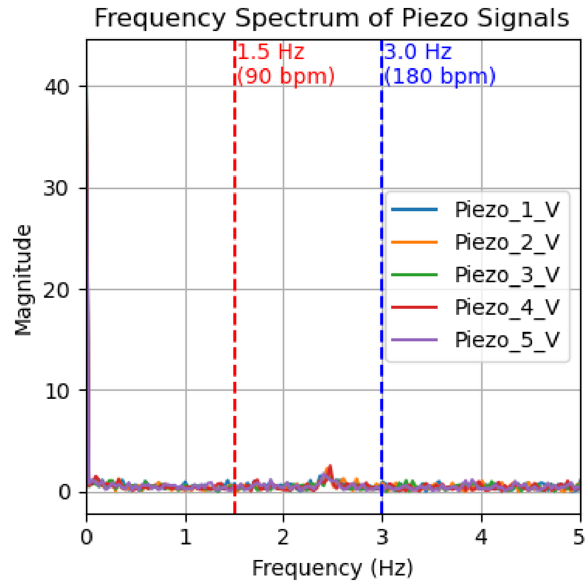

Fig. 3. Frequency Spectrum of Raw Piezoelectric Sensor Signals. Fourier-transformed voltage signals recorded from five piezoelectric sensors during a representative trial (Trial #1: Pairing of 147 BPM and 142 BPM). Vertical dashed lines at 1.5 Hz (90 bpm) and 3.0 Hz (180 bpm) indicate the lower and upper bounds of the target frequency band for fetal heart rate detection. Most signal energy is concentrated between these cutoffs, consistent with the expected physiological range.

fourth-order Butterworth bandpass filter with cutoff frequencies of 1.5 Hz and 3.0 Hz was implemented to restrict the signals to a frequency range corresponding to heart rates between 90 and 180 beats per minute. This a broader range was chosen to encompass the normal fetal heart rate range (approximately 110–160 beats per minute) while also accounting for potential cases of fetal bradycardia (heart rate <110 bpm) and tachycardia (heart rate >160 bpm). This filtering step effectively attenuated low-frequency baseline drift and high-frequency noise, as verified by inspection of the pre-filtered frequency spectra (Figure 4). Following bandpass filtering, a frequency-domain magnitude thresholding procedure was performed. Specifically, the filtered signals were

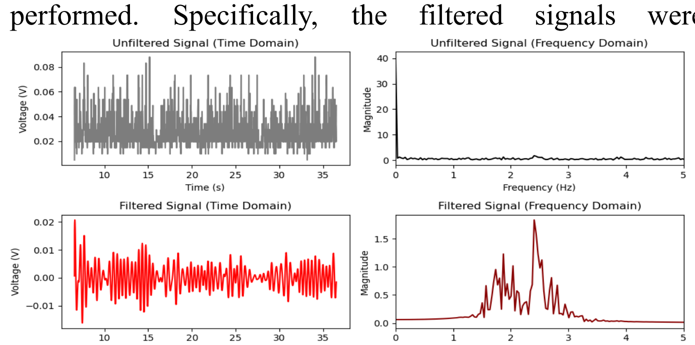

Fig. 4. Comparison of Unfiltered and Filtered Signals from Piezoelectric Sensor #5. Time- and frequency-domain representations of unfiltered and filtered voltage signals recorded from Piezoelectric Sensor #5 during a representative trial (Trial 1: 147 BPM and 142 BPM pair). Top panels show the raw, unfiltered signal; bottom panels show the corresponding signal after bandpass filtering. Filtering enhances the clarity of the oscillatory components around the target frequencies.

transformed into the frequency domain using a real fast Fourier transform (rFFT), and frequency components with magnitudes below a set threshold were zeroed. An inverse rFFT was subsequently applied to reconstruct the time-domain signals, further suppressing spurious noise contributions outside the target band. The resulting filtered signals preserved the dominant physiological components while minimizing artifacts, as demonstrated by comparative analysis of the time- and frequency-domain representations before and after filtering (Figure X).

Accuracy of Fetal Heart Rate Estimation

Voltage signals from five piezoelectric sensors were analyzed to estimate the dominant frequencies of two concurrent fetal heart rate sources. As detailed in the methods section, a two-component GMM differentiates and reconstructs two fetal heart beat sources using the extracted TDOA features (Supplementary Figure 2). Frequency estimation accuracy was quantified by comparing the dominant estimated frequencies to the known ground truth values, with percent errors reported for each cluster (Figure 5). The accuracy of fetal heart rate (FHR) estimation was assessed across all pairing conditions by calculating the average percent error between the estimated and true frequencies over three trials per pairing.

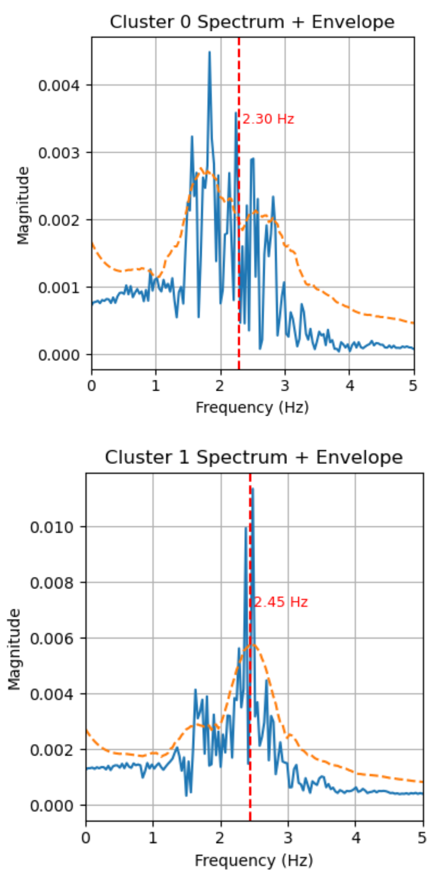

Fig. 5. Frequency Spectra and Envelope Curves for Clustered FHR Signals. Power spectra with overlaid Hilbert envelope (orange dashed) for Cluster 0 (top) and Cluster 1 (bottom) extracted from a representative trial (Trial #1: Pairing of 147 BPM and 142 BPM). The vertical red dashed lines indicate the dominant frequency peaks of 2.45 Hz (Cluster 1) and 2.30 Hz (Cluster 0), corresponding to estimated fetal heart rates.

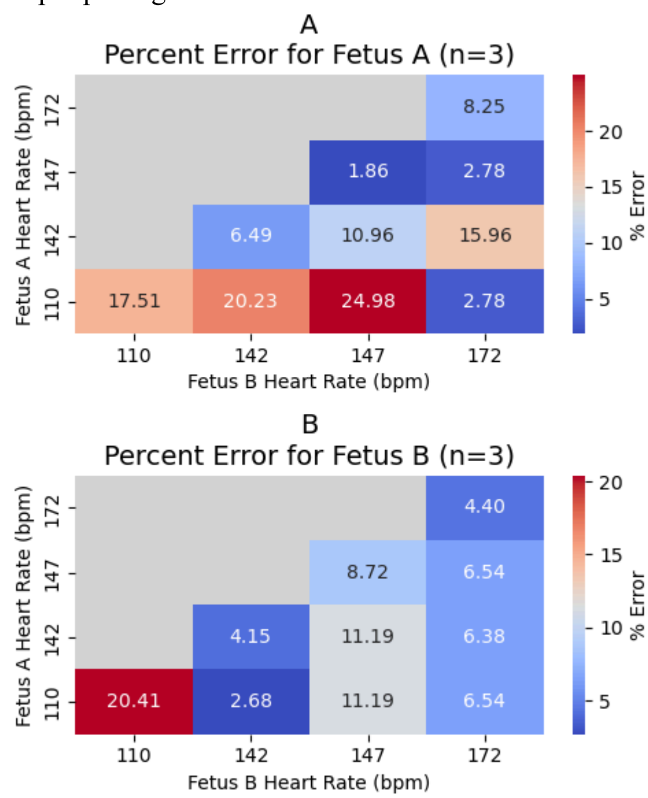

Fig. 6. Percent Error Heatmaps for Fetal Heart Rate Estimation. Heatmaps showing the average percent error in estimated fetal heart rates across ten pairing conditions, with three trials per condition. (A) displays error for Fetus A, and (B) for Fetus B, across varying true heart rates (110, 142, 147, 172 bpm). Gray cells indicate untested symmetric or duplicate combinations.

Heatmaps summarizing the average percent error for each source (Fetus A and Fetus B) are shown in Figure 6. For Fetus A, the lowest average percent errors (<3%) were observed when paired with heart rates of 172 bpm and 142 bpm (e.g., 172&147 and 147&172 combinations), indicating robust frequency separation when heart rates were well separated or moderately close but not identical. However, significantly higher errors (up to 24.98%) occurred when Fetus A was paired with itself or with close neighboring rates (e.g., 110&147, 110&142), suggesting difficulty distinguishing sources with overlapping or similar frequencies. Similarly, for Fetus B, estimation errors were generally low (<7%) across most pairings, but errors increased (up to 20.41%) when both sources had low heart rates (110 bpm). Notably, asymmetric trends were observed between Fetus A and Fetus B: Fetus B exhibited lower percent errors overall, particularly when paired with higher-frequency sources. These results demonstrate that FHR estimation accuracy is highly dependent on the separation between source heart rates, with lower errors achieved when the two fetal signals are either distinctly different or sufficiently separated in frequency space. The presence of high errors in cases involving 110 bpm suggests that low-frequency sources are more prone to clustering and frequency estimation ambiguities.

Accuracy of Fetal Heart Source Localization

Localization error was quantified as the average Euclidean distance between the estimated and true source locations for each speaker across all trials. Specifically, for each source (A and B), the estimated (x, y) coordinates obtained from multilateration or grid search were compared to the known true (x, y) coordinates. The mean error radius for each source was calculated by averaging the individual errors across all trials. These mean radii were used to draw error circles centered at the true source locations, representing the average localization uncertainty.

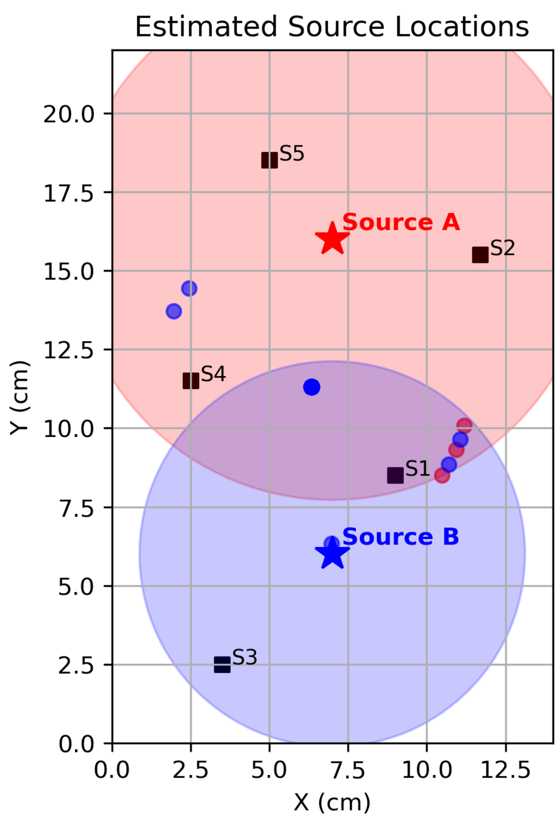

Fig. 7. Estimated Source Locations and Localization Error Regions. Localization results showing estimated positions of two sound sources (Source A in red, Source B in blue) relative to five piezoelectric sensors (S1–S5, black squares). Colored circles represent localization error bounds (maximum deviation from the true position) for each source, derived from multiple trial estimates. Clustered estimations (red and blue circles) tend to show higher variance for Source A, suggesting greater uncertainty or signal overlap in that region. Overlap of the error regions indicates spatial ambiguity in source separation.

Figure 7 demonstrates that estimates for Source B are generally more tightly clustered around the true location compared to Source A, suggesting slightly better localization precision for lower-positioned sources within the hydrogel. The sensor array configuration and true source placements influence the spread and bias of the localization estimates, with larger deviations observed for sources located farther from the sensor centroid. In particular, some location estimates fell outside the physical boundary of the hydrogel phantom, causing the mean error circles to not fully encompass all estimated points. This reflects the compounded effect of TDOA measurement errors and boundary limitations on localization performance.

Discussion

The FHR triangulation system developed in this study demonstrates the feasibility of differentiating and localizing multiple heart sources within a hydrogel phantom that mimics the uterine environment. By using piezoelectric sensors arranged in a randomized, non-collinear array, our design minimized geometric degeneracy and improved source separation accuracy. The integration of Gaussian Mixture Models and multilateration algorithms enabled the system to effectively distinguish between two concurrent heart signals, particularly when the frequencies were distinctly different or far apart.

Despite these successes, several limitations were identified. FHR estimation accuracy declined when signals approached each other in frequency space, particularly around 110 bpm, suggesting a sensitivity to low-frequency overlap and noise. Localization accuracy averaged 6–8 cm but decreased when sources were placed farther from the array centroid, reflecting boundary effects and uneven sensor coverage. These challenges point to the need for denser or dynamically adjustable sensor configurations in future iterations.

While the current system performed well in a controlled phantom model with stationary sources, further development is needed to transition toward clinical application. Future designs should incorporate maternal heart signals to improve signal discrimination, especially in late gestation when fetal and maternal heartbeats can overlap. Additionally, validation in dynamic environments, such as fetal movement or maternal motion, will be critical. With refinement, this novel monitoring approach has the potential to enhance clinical care for twin pregnancies by improving diagnostic precision, enabling timely interventions, and ultimately reducing complications associated with inaccurate FHR monitoring.

End Matter

Author Contributions and Notes
The authors declare no conflict of interest.

Code Availability
The code repository supporting this study is available on public GitHub repository: https://github.com/CarolWuuu/Capstone25.git

Acknowledgments
Dr. Kristen Naegle, PhD, Associate Professor, Biomedical Engineering
Dr. Natasha Sheybani, PhD, Assistant Professor of Biomedical Engineering
Dr. Christopher Ennen, MD, Assistant Professor, Maternal - Fetal Medicine
Capstone Teaching Team (Dr. Allen, Mario Garcia, Hayley Sussman)

References

1. FastStats. https://www.cdc.gov/nchs/fastats/multiple.htm (2024).
2. FOTSO, J. C., CLELAND, J., MBERU, B., MUTUA, M. & ELUNGATA, P. BIRTH SPACING AND CHILD MORTALITY: AN ANALYSIS OF PROSPECTIVE DATA FROM THE NAIROBI URBAN HEALTH AND DEMOGRAPHIC SURVEILLANCE SYSTEM. *J. Biosoc. Sci.* **45**, 779–798 (2013).
3. Meitern, R., Gortfelder, M., Puur, A. & Hõrak, P. Mothers of twins had higher old-age survival than mothers of singletons in Estonian 19th-century birth cohorts. *Hum. Reprod. Oxf. Engl.* **39**, 2124–2133 (2024).
4. Dudenhausen, J. W. & Maier, R. F. Perinatal Problems in Multiple Births. *Dtsch. Ärztebl. Int.* **107**, 663–668 (2010).
5. Marzbanrad, F., Stroux, L. & Clifford, G. D. Cardiotocography and Beyond: A Review of One-Dimensional Doppler Ultrasound Application in Fetal Monitoring. *Physiol. Meas.* **39**, 08TR01 (2018).
6. Normal Endometrial Thickness for Pregnancy. https://www.cloudninecare.com/blog/endometrium-thickness-in-pregnancy-symptoms-treatment.

Supplementary Material

Supplementary Figure 1. Image of the Gel Phantom Setup.

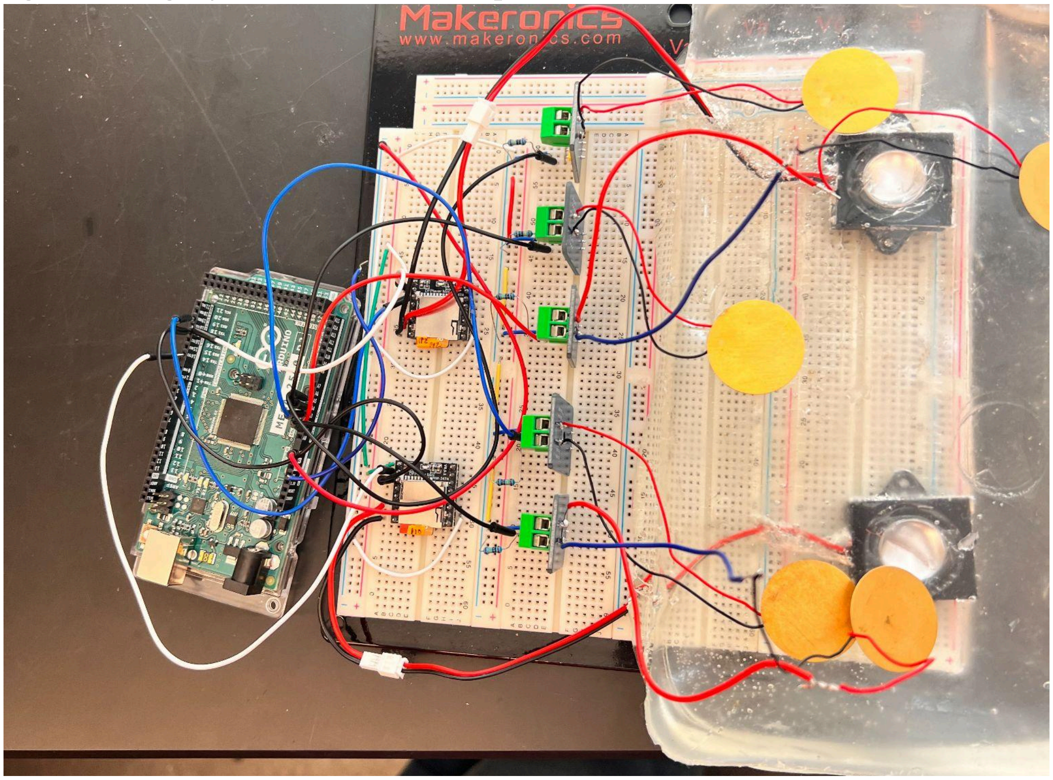

Supplementary Table 1. Reference Audio Sources for Synthetic Fetal Heartbeat Frequencies. *Links to fetal heartbeat recordings used to generate synthetic heart rate signals in the experimental trials. The table includes beats per minute (BPM) values and corresponding audio sources. Heartbeats at 142 BPM and 147 BPM were based on publicly available fetal Doppler recordings representing typical third-trimester fetal heart rates. All recordings are available in the GitHub Repository.*

Fetal Heartbeat (BPM)	**Recording Drive Link**
110	https://www.youtube.com/shorts/ltOxsIKSVfs
142	https://www.youtube.com/watch?v=MTrBC7MP4rk (used fetal heart beat sounds at 35 weeks)
147	https://www.youtube.com/watch?v=32JCR69CJvo
172	https://www.youtube.com/watch?v=lNqEA1POohg

Supplementary Table 2. Materials Used in Fetal Heart Rate Monitoring System. *List of key components used in the fetal heart rate detection system, including electronic modules, acoustic hardware, prototyping materials, and the hydrogel phantom. Each item includes a link source and brief description of its specifications or use case in the experimental setup.*

Material	Link	Description
Arduino Mega 2560 Rev3	Arduino-store	The 8-bit board with 54 digital pins, 16 analog inputs, and 4 serial ports.
Speakers	Amazon-square	4 PCS Speaker 3 Watt 8 Ohm Mini Speaker 8ohm 3w Loundspeaker Micro Speaker for Arduino with JST-PH2.0 Interface for Small Electronic Projects Advertising Machines LCD TV Monitors
Breadboard + Jump wires	Amazon	Makeronics Solderless 3220 Breadboard Complete Kit-3220 Tie-Points Experiment Plug-in Breadboard with Aluminum Back Plate +560 U-Shape|65 PCS Pure Copper Jumper Wires for Prototyping Circuit/Arduino
Resistors + capacitors	Amazon - resistor + capacitor	1400Pcs Basic Electronics Component Assortment Kit, Electrolytic Capacitor, Ceramic Capacitor, LED Diode, Common Diode, Resistor, Transistor Component for Arduino, Electronic DIY Project
Hydrogel #3	hydrogel	Gelatin #3 – Medical Gel By The Pound || One pound equals 32 cubic inches Density: of 856.839ρ [Kg/m^3] Speed of Sound: 1458.85 [m/s] Young's Modulus: 0.19 [MPa]
Piezoelectric	Amazon	Gikfun Analog Ceramic Piezo Vibration Sensor Module for Arduino DIY Kit EK 1952 , 5 Volts, 3.3 Volts, 1.18"W x 0.91"H
TF card	Amazon	2 Pack TF Card 8GB with Adapter, High Speed Memory Card, UHS-I C10 A1 Memory TF Card for Tablet/Mobile Phone/Camera/Car Audio/Game Console (TF162 Red Gold 8GB)
DFPlayer	Amazon	HiLetgo 2pcs mp3 Player Mini MP3 Player Audio Voice Module TF Card U Disk Board for DFPlayer Audio Voice Music Module

Supplementary Figure 2. Reconstructed Source Signals Using TDOA-Based Clustering. *Time-domain reconstruction of two source signals separated using Time Difference of Arrival (TDOA) features and Gaussian Mixture Model clustering. Cluster 0 (blue) and Cluster 1 (orange) represent the demixed waveforms corresponding to two synthetic fetal heartbeats in a representative trial (Trial #1: Pairing of 147 BPM and 142 BPM).). The signals demonstrate temporal overlap but distinct waveform patterns, supporting successful source separation despite close frequency content.*

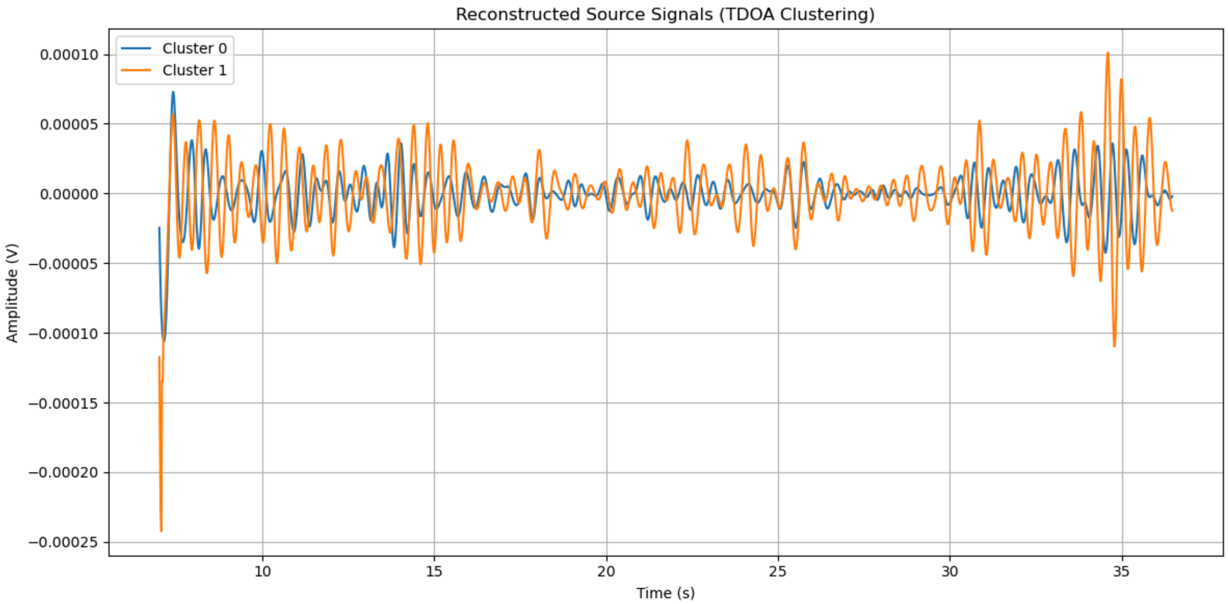

Supplementary Table 3. Estimated Frequencies and Percent Errors for Fetal Heart Rate (FHR) Pairings Across Trials. *True and estimated frequencies for each speaker across FHR signal pairings, with corresponding percent errors. Each condition includes three estimates per speaker. FHRs are labeled by pair (e.g., 1–1, 1–2), where numerals indicate distinct synthetic heartbeat frequencies.*

FHR Pair	Speaker	True Freq (Hz)	Est. Freq (Hz)	Freq % Error
1-1	A	2.45	2.5	2.05
			2.264	0.85
			2.515	2.67
	B	2.45	2.535	3.45
			2.08	15.11
			2.264	7.6
1-2	A	2.45	2.504	2.21
			2.576	5.16
			2.426	0.98
	B	2.867	2.805	2.18
			2.728	4.85
			2.506	12.58
1-3	A	2.375	2.296	3.32

			2.669	12.39
			2.783	17.18
	B	2.45	2.449	0.04
			2.871	17.17
			2.851	16.36
1-4	A	1.833	2.557	39.47
			1.991	8.62
			2.325	26.84
	B	2.45	2.648	8.07
			2.252	8.08
			2.389	2.5
2-2	A	2.867	2.779	3.05
			2.415	15.76
			2.7	5.94
	B	2.867	2.779	3.05
			2.746	4.21
			2.7	5.94
2-3	A	2.375	2.647	11.46
			2.656	11.82
			1.791	24.59
	B	2.867	2.699	5.86
			2.682	6.45
			2.671	6.84
2-4	A	1.83	2.332	27.2
			1.781	2.84
			1.881	2.63
	B	2.867	2.64	7.91
			2.375	17.17
			2.08	27.39
3-3	A	2.375	2.197	7.49
			2.16	8.91
			2.448	3.06
	B	2.375	2.437	2.63
			2.501	5.32
			2.482	4.49

3-4	A	1.833	2.356	28.55
			2.033	10.91
			2.222	21.24
	B	2.375	2.39	0.65
			2.219	6.56
			2.395	0.82
4-4	A	1.833	2.441	33.17
			2.076	13.28
			1.722	6.07
	B	1.833	2.472	34.85
			2.298	25.37
			1.852	1.02

Supplementary Table 4. Estimated Speaker Locations Across Fetal Heart Rate (FHR) Pairing Trials.

Pair	Trial	Speaker	Est. X (cm)	Est. Y (cm)
1&1	t1	A	6.34	11.3
1&1	t1	B	1.96	13.71
1&1	t2	A	6.34	11.3
1&1	t2	B	11.06	9.65
1&1	t3	A	-14.99	82.13
1&1	t3	B	6.34	11.3
1&2	t1	A	6.34	11.3
1&2	t1	B	6.34	11.3
1&2	t2	A	6.34	11.3
1&2	t2	B	6.34	11.3
1&2	t3	A	6.34	11.3
1&2	t3	B	6.34	11.3
1&3	t1	A	6.34	11.3
1&3	t1	B	6.34	11.3
1&3	t2	A	6.34	11.3
1&3	t2	B	6.34	11.3
1&3	t3	A	6.34	11.3

1&3	t3	B	6.34	11.3
1&4	t1	A	6.34	11.3
1&4	t1	B	6.34	11.3
1&4	t2	A	10.49	8.51
1&4	t2	B	6.34	11.3
1&4	t3	A	-0.21	23.73
1&4	t3	B	6.34	11.3
2&2	t1	A	6.34	11.3
2&2	t1	B	6.34	11.3
2&2	t2	A	10.93	9.32
2&2	t2	B	6.34	11.3
2&2	t3	A	6.34	11.3
2&2	t3	B	6.34	11.3
2&3	t1	A	6.34	11.3
2&3	t1	B	6.34	11.3
2&3	t2	A	6.34	11.3
2&3	t2	B	6.34	11.3
2&3	t3	A	6.34	11.3
2&3	t3	B	6.34	11.3
2&4	t1	A	6.34	11.3
2&4	t1	B	6.34	11.3
2&4	t2	A	6.34	11.3
2&4	t2	B	6.34	11.3
2&4	t3	A	-1.41	15.44
2&4	t3	B	6.34	11.3
3&3	t1	A	17.42	8.84
3&3	t1	B	6.34	11.3
3&3	t2	A	7.67	32.26
3&3	t2	B	6.34	11.3
3&3	t3	A	6.34	11.3

3&3	t3	B	6.98	6.34
3&4	t1	A	6.34	11.3
3&4	t1	B	6.34	11.3
3&4	t2	A	-0.85	15.27
3&4	t2	B	6.34	11.3
3&4	t3	A	6.34	11.3
3&4	t3	B	2.45	14.44
4&4	t1	A	11.19	10.08
4&4	t1	B	6.34	11.3
4&4	t2	A	6.34	11.3
4&4	t2	B	10.69	8.84
4&4	t3	A	6.34	11.3
4&4	t3	B	9.79	32.01